nature geoscience

LETTERS

PUBLISHED ONLINE: 17 NOVEMBER 2014 | DOI: 10.1038/NGEO2291

Important role for organic carbon in subduction-zone fluids in the deep carbon cycle

Dimitri A. Sverjensky[1]*, Vincenzo Stagno[2] and Fang Huang[1]

Supercritical aqueous fluids link subducting plates and the return of carbon to Earth's surface in the deep carbon cycle[1,2]. The amount of carbon in the fluids and the identities of the dissolved carbon species are not known, which leaves the deep carbon budget poorly constrained[3]. Traditional models[4,5], which assume that carbon exists in deep fluids as dissolved gas molecules, cannot predict the solubility and ionic speciation of carbon in its silicate rock environment. Recent advances enable these limitations to be overcome when evaluating the deep carbon cycle[6–8]. Here we use the Deep Earth Water theoretical model[7] to calculate carbon speciation and solubility in fluids under upper mantle conditions. We find that fluids in equilibrium with mantle peridotite minerals generally contain carbon in a dissolved gas molecule form. However, fluids in equilibrium with diamonds and eclogitic minerals in the subducting slab contain abundant dissolved organic and inorganic ionic carbon species. The high concentrations of dissolved carbon species provide a mechanism to transport large amounts of carbon out of the subduction zone, where the ionic carbon species may influence the oxidation state of the mantle wedge. Our results also identify novel mechanisms that can lead to diamond formation and the variability of carbon isotopic composition via precipitation of the dissolved organic carbon species in the subduction-zone fluids.

Supercritical aqueous fluids released from subducting plates carry distinctive suites of elements, including carbon, and have long been invoked to trigger partial melting[9], oxidation of the mantle wedge overlying subduction zones[10,11], and mantle metasomatism and diamond formation[11]. However, quantitative theoretical models linking ionic species in the fluids to the rock chemistry are lacking. Instead, aqueous fluids in the deep crust and upper mantle have long been modelled as a mixture of neutral gas molecules—such as CO_2, CH_4 and H_2O (that is, COH fluids)—without consideration of aqueous ions[4,5]. In such models, the pH values and bicarbonate or carbonate ion concentrations of subduction-zone fluids are not known. Dehydration and decarbonation reactions alone are invoked for C mobility in fluids, leading to an inability to explain why so much C is degassed over subduction zones[1,3]. As a result, the involvement of aqueous fluids in the deep carbon cycle remains enigmatic.

Recent studies of carbonate rock dissolution in subduction zones, fluid inclusions in diamonds, solubility and ionic speciation experiments, and theoretical calculations[1,2,6,12–14] have indicated that aqueous carbonate or bicarbonate ions may play a role in the transport of carbon in the deep Earth carbon cycle. However, none of these studies have quantified C-solubilities or C-speciation in equilibrium with silicate minerals. As the solubility and speciation can be expected to depend on the nature of the silicate environment in the deep crust or upper mantle, it is crucial to include silicate minerals when evaluating the deep carbon cycle. Here we use the new Deep Earth Water (DEW) model[7], enabling theoretical calculation of equilibrium constants involving aqueous ions, metal complexes, neutral species and minerals to 6 GPa and 1,200 °C (Methods). In turn, this permits calculation of aqueous C-speciation (including organic species such as aliphatic acids and hydrocarbons with a greater number of C atoms than methane) and solubility models in equilibrium with silicate mineral assemblages under upper mantle conditions.

New predictions of aqueous C-speciation are given in Fig. 1a,b. At relatively low pressures (Fig. 1a), only the most reduced and oxidized forms of aqueous carbon are stable. In contrast, at high pressures (Fig. 1b), acetic acid and acetate fields lie between the quartz–fayalite–magnetite (QFM) and Fe–FeO (iron–wustite (IW)) redox buffers representative of the upper mantle[11], and near neutral pH. For the sake of simplicity, only the species shown were considered. Nevertheless, this example demonstrates that acetic acid and acetate with carbon in an overall oxidation state of zero can coexist with CO_2 (+IV) and CH_4 (−IV) at full chemical equilibrium. A rich variety of aqueous organic and inorganic carbon species can be expected at high pressures without the metastable equilibria of shallow crustal conditions[15].

We now consider (Fig. 2a,b) how this new carbon speciation depends on pressure in upper mantle silicate rocks. It can be seen that the field for acetate predominance at 600 °C is restricted to pressures greater than about 2.9 GPa. Calculations at higher temperatures indicate that at 800 °C the lower pressure limit for acetate increases to about 3.9 GPa, and that by 1,000 °C the field for acetate disappears.

Superposed on Fig. 2a,b are indications of the pH ranges to be expected in upper mantle environments (Methods). Abundant evidence for carbon in both eclogitic and peridotitic environments comes from studies of inclusions in diamonds[16] and experimental studies of carbonates in eclogites[17]. Therefore, we consider aqueous fluids in equilibrium with minerals in eclogitic and peridotitic environments. The pairs of dashed lines in Fig. 2a represent a pH range for a model metasedimentary eclogitic assemblage approximated by jadeite + kyanite + coesite[18], whereas in Fig. 2b the dashed lines refer to a model mafic eclogitic assemblage approximated by jadeite + pyrope + coesite + talc[18]. In both figures, the solid line segment represents a range of pH values corresponding to a model peridotitic assemblage approximated by forsterite + orthoenstatite.

A clear difference between eclogitic and peridotitic fluids can be seen in Fig. 2a,b. Eclogitic fluids contain dissolved organic carbon species such as aliphatic acid anions with zero oxidation state, depending on the P–T path during subduction. However,

[1]Department of Earth and Planetary Sciences, Johns Hopkins University, Baltimore, Maryland 21218, USA. [2]Geophysical Laboratory, Carnegie Institution of Washington, Washington DC 20015, USA. *e-mail: sver@jhu.edu

© 2014 Macmillan Publishers Limited. All rights reserved.

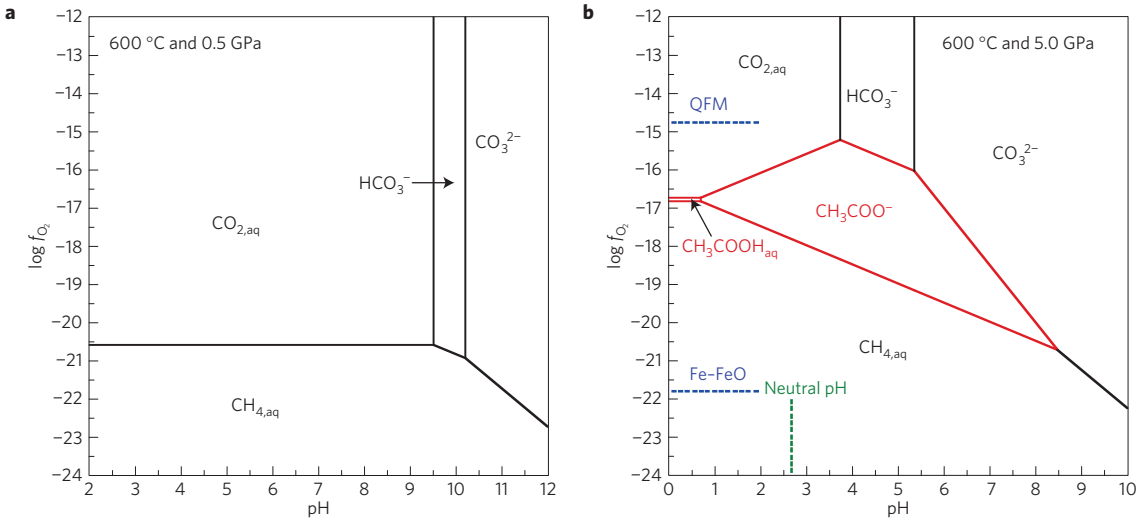

Figure 1 | Predicted log f_{O_2} versus pH diagrams for aqueous C-species constructed using equilibrium constants calculated with the DEW model. a, At 600 °C and 0.5 GPa, only the usual carbonate species and methane are stable. **b**, At 600 °C and 5.0 GPa, equilibrium stability fields appear for aqueous organic species acetic acid and acetate.

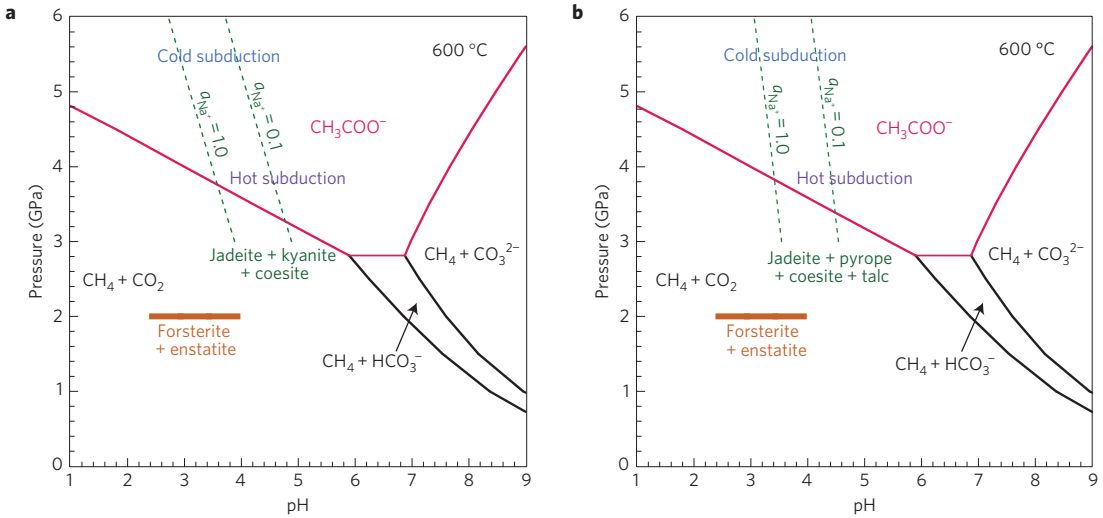

Figure 2 | Pressure-dependent stability of an organic acid anion versus aqueous phase pH. a, Comparison of peridotitic and metasedimentary eclogitic fluids. **b**, Comparison of peridotitic and mafic eclogitic fluids. It can be seen that the aqueous acetate stability field appears only at pressures above approximately 2.9 GPa at 600 °C.

peridotitic fluids contain dissolved carbon present as CO_2 or CH_4, depending on the oxidation state, consistent with traditional COH fluid models[5]. Our model is able to predict this difference between the two fluids because it includes aqueous ions (Methods), whereas the traditional COH fluid models do not include ions.

We have also carried out full aqueous C-speciation calculations for model eclogitic and peridotitic mineral assemblages (Methods). In these calculations, a total of 21 aqueous C-species were considered in the aqueous speciation model (Supplementary Information) and the fluid chemistry is completely coupled to the mineral assemblages. As a first approximation, it is assumed that the pH is constrained by pure silicate minerals, which does not significantly affect the results (Methods). However, the aqueous C-speciation is strongly affected by the log f_{O_2} values. Recent progress in quantifying the log f_{O_2}–P–T conditions in upper mantle peridotites and eclogites using experimental data[19,20] and natural samples[21] suggests that log f_{O_2} may range from about QFM to QFM−4.0 at pressures up to 7.0 GPa based on the Fe^{3+} content of garnet in redox-sensitive equilibria with olivine, orthopyroxene and clinopyroxene.

For eclogitic fluids, we show in Fig. 3 the predicted aqueous carbon speciation in equilibrium with diamond, jadeite, pyrope, kyanite and coesite at QFM−2.0 at 5 GPa and a range of temperatures, from cold to hot subduction-zone conditions[22]. The total dissolved carbon concentrations at 600, 700, 800, 900 and 1,000 °C are 0.03, 0.2, 1, 4 and 20 molal (moles per kg, m), respectively. Concentrations of about 1 m dissolved C at the higher temperatures are about an order of magnitude greater than those needed to oxidize the mantle wedges above subduction zones[10]. Only the most abundant aqueous C-species are shown in Fig. 3. Particularly striking are the organic species propionate and formate, in redox equilibrium with CO_2 and CH_4. The most important overall result of these calculations is that large amounts of aliphatic organic species may be stable with CO_2 and CH_4 at elevated pressures in deep crustal and upper mantle eclogitic fluids provided that the oxidation state is about QFM−2.0 units[20].

For peridotitic fluids, we carried out aqueous speciation calculations along a representative mantle geotherm corresponding to a heat flow of 42 mW m^{-2} (Fig. 4a). The log f_{O_2} values shown

© 2014 Macmillan Publishers Limited. All rights reserved.

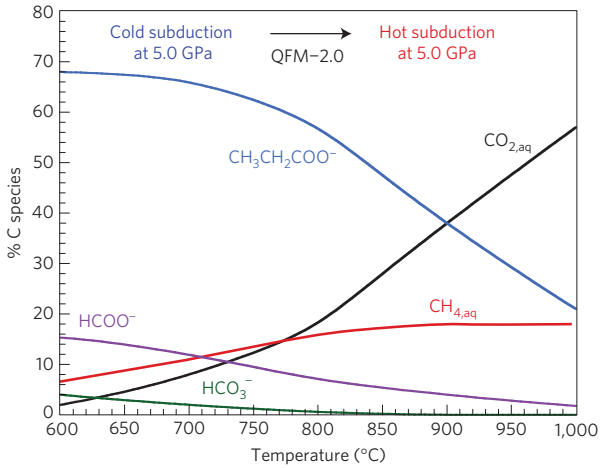

Figure 3 | Aqueous C-speciation in equilibrium with a model metasedimentary eclogite containing diamond, jadeite, pyrope, kyanite, and coesite. At 5.0 GPa a range of temperatures is considered, from cold to hot subduction zones. Ionic organic carbon species such as propionate are predicted to be abundant in the subduction-zone fluids.

represent the midpoints of calculated values corresponding to a range of 5–10% Fe^{3+} in garnet. These values of ferric iron content are representative of natural garnet-bearing mantle xenoliths that experienced interaction with graphite, diamond, carbonate minerals or carbonatitic liquids[19,23]. The mineral assemblages used to fix the pH and aqueous speciation are also shown. It was further assumed that the fluid contained 1.0 m Cl and 1.0 m C—that is, the fluids were undersaturated with respect to graphite and diamond. The calculated speciation of carbon is shown in Fig. 4b. A transition from CO_2-dominant to CH_4-dominant fluids occurs at about 100 km depth and a predicted log f_{O_2} of −1 to −2 relative to QFM. This is qualitatively consistent with the traditional COH fluid picture[5].

There are two main reasons for the differences in C-speciation between eclogitic and peridotitic fluids. First, the temperatures considered at 5 GPa for the eclogitic fluids are significantly lower than the corresponding temperature of 1,140 °C at 5 GPa along the lithospheric mantle geotherm of the peridotitic environment. The lower temperatures favour dissociation of CO_2 and polymerization of carbon. Second, the pH values of the eclogitic fluids are strongly alkaline, which again favours ionic C-bearing species. It should be emphasized here that the eclogitic fluids discussed here may be at conditions above the second critical endpoint[24]. They contain significant amounts of solutes (Supplementary Information), but these may be underestimates given the likelihood of complex polymerized Si-bearing species at high pressures[8,24].

Our calculations suggest that large concentrations of dissolved carbon could be present as ionic organic species in aqueous fluids in the upper mantle. The C-species in deep fluids are not restricted to the oxidation states of +IV and −IV. These results have important implications for the deep carbon cycle. First, substantial amounts of carbon could be emitted from subducting plates at sub-arc depths by aqueous fluids. Fluids from hot subduction zones, in particular, could carry enough carbon to be involved in oxidation of the mantle wedge. Although other elements such as Fe or S may also be involved in this process[10], the present results provide preliminary theoretical support for the hypothesis that dissolved C-species are sufficiently abundant to play a role in mantle oxidation[2].

Second, new mechanisms arise for the formation and the isotopic composition of diamond. Diamond may form in the sub-cratonic lithospheric mantle when metasomatic fluids from subducting plates encounter peridotite[16]. Traditional models always invoke redox changes, such as the oxidation of CH_4 or the reduction of CO_2 (or carbonate-bearing melts). But our results suggest that diamond may precipitate from fluids containing organic C-species as in

$$CH_3COO^- + H^+ \rightarrow 2C_{diamond} + 2H_2O$$

The carbon in acetate has the same zero oxidation state as diamond. No redox change is needed. Instead, pH changes associated with metasomatic reactions in the silicate rock environment could induce diamond precipitation (Supplementary Information). Such reactions were not conceptually possible using the traditional COH model of upper mantle fluids.

The importance of pH as well as f_{O_2} in determining the C-species in deep fluids strongly suggests that both variables should influence the carbon isotopic compositions of diamond. This dependence was suggested long ago for graphite in shallow crustal hydrothermal systems[25]. However, it has not been possible to apply this concept to diamond until now. It is now clear that a wide spectrum of aqueous C-species and their isotopic fractionations in deep fluids need to be considered as a function of aqueous fluid chemistry. For example, if diamond precipitates from acetate, the isotopic fractionation between the two should be small because there is no difference in C-oxidation state. In this instance, the isotopic composition of the diamond reflects that of the acetate, which may, however, be different from the total C-isotopic composition of the fluid. Much more needs to be done experimentally to determine the appropriate fractionation factors.

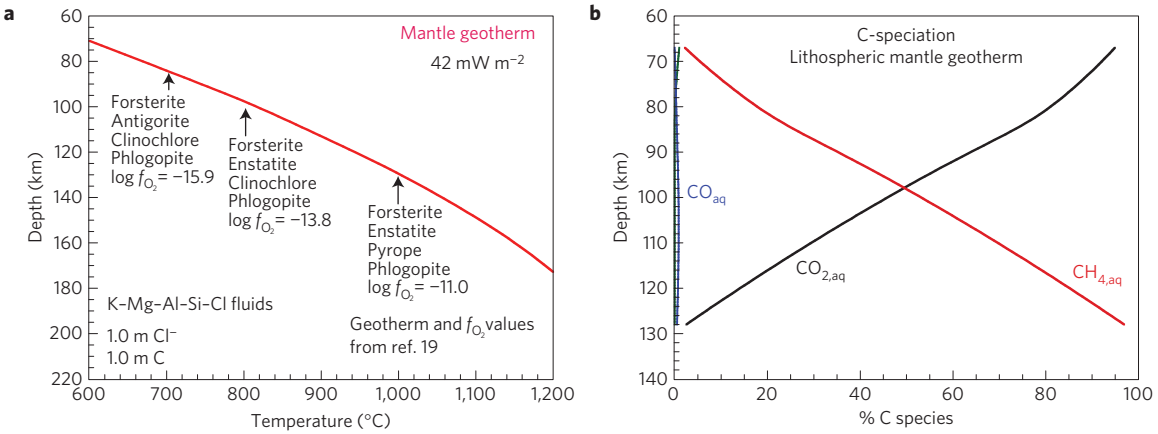

Figure 4 | Aqueous C-speciation in peridotitic fluid containing 1.0 m C and Cl. a, Mantle geotherm, mineral assemblages and oxidation state. **b**, Predicted aqueous carbon species consist of the traditional COH fluid species.

© 2014 Macmillan Publishers Limited. All rights reserved.

Finally, our results suggest a new connection between the shallow and deep carbon cycles. In eclogitic fluids ascending in Earth's crust, aliphatic acid anions, and more complex C-bearing species, might become metastable as the kinetics of equilibration slow at lower temperatures. Such metastability could lead to the persistence of a wide variety of aqueous, liquid and solid hydrocarbon species in the crust (for example, 'hydrogenated carbon' as inclusions in diamonds from ultrahigh-pressure metamorphic rocks[21]). Ascending fluids carrying a complex suite of C-bearing species might also provide a source of energetically attractive molecules for the deep biosphere at present or on early Earth.

Methods

The DEW model[7] for calculating the standard Gibbs free energies of aqueous species at high pressures was used. The DEW model is based on an extension of the Helgeson–Kirkham–Flowers (HKF) aqueous species equation of state, traditionally limited to an upper pressure of 0.5 GPa because of lack of knowledge of the dielectric constant of water at high pressures[26]. We have taken advantage of recent experimental and theoretical advances[7,12] that enable this limitation to be overcome, and shown that the HKF formalism can be applied to experimental solubility and aqueous speciation data for quartz, forsterite + enstatite, corundum, calcite and aragonite at pressures up to 6.0 GPa (ref. 6), enabling theoretical predictions of equilibrium constants involving aqueous inorganic and organic ions, and neutral species and metal complexes up to pressures and temperatures of the upper mantle. Overall uncertainties in the DEW model may be of the order of ±0.3–0.5 units in equilibrium constants for aqueous species at high temperatures and pressures[7]. However, it should be emphasized that all the aqueous species used in our calculations rest on experimental calibrations for as wide a range of temperatures or pressures as is available. A key feature of all the calculations reported below is that HCl is a component of each chemical system considered. This is what enables ionic species to be considered in the models[27].

The boundaries between the aqueous species shown in Figs 1 and 2 were calculated using predicted equilibrium constants and unit activities of each aqueous species. For simplicity, only the species CO_2, HCO_3^-, CO_3^{2-}, CH_4, CH_3COOH, CH_3COO^- were considered in Figs 1 and 2. In Fig. 1b, neutral pH is indicated, based on the calculated value of the dissociation constant of water. In Fig. 2a,b, the solid line labelled forsterite + enstatite represents an approximation of the range of pH values expected for aqueous fluid in equilibrium with peridotite. Assuming equilibrium between aqueous fluid, Mg-rich olivine and orthopyroxene enables one to write

$$Mg_2SiO_4 + 2H^+ = MgSiO_3 + Mg^{2+} + H_2O \quad (1)$$

for which the equilibrium constant (K) and thermodynamic activities of the ith species (a_i) can be written as

$$\log K = \log \frac{a_{Mg^{2+}}}{a_{H^+}^2} \quad (2)$$

Assuming unit activities of the minerals and water in equation (2) gives

$$pH = \frac{1}{2}\log K - \frac{1}{2}\log a_{Mg^{2+}} \quad (3)$$

Values of $\log K$ were calculated using standard Gibbs free energies of the aqueous species, as described above, together with standard Gibbs free energies of forsterite and orthoenstatite[28]. Alternative values for the Gibbs free energies of these minerals from other thermodynamic databases[29] did not give significantly different results for the purposes of Fig. 2a,b. A range of values for the $a_{Mg^{2+}}$ from 0.001 to 1.0 was used in equation (3), resulting in a range of estimated pH values. Taking into account solid solutions would decrease the activities of the minerals in equation (1), resulting in shifts in the pH of about 0.1–0.2, which is small compared to the range of pH associated with the range of $a_{Mg^{2+}}$ values.

Also in Fig. 2a,b, the dashed lines labelled jadeite + kyanite + coesite and jadeite + pyrope + coesite + talc represent approximations of the possible range of pH values expected for fluids in equilibrium with metasedimentary and mafic eclogites, respectively. For the metasedimentary eclogite, equilibrium between the aqueous fluid, omphacitic clinopyroxene, kyanite and coesite enables one to write the following:

$$2NaAlSi_2O_6 + 2H^+ = Al_2SiO_5 + 3SiO_2 + 2Na^+ + H_2O \quad (4)$$

for which

$$\log K = \log \frac{a_{Na^+}^2}{a_{H^+}^2} \quad (5)$$

Unit activities of the minerals and the water in equation (5) gives

$$pH = \frac{1}{2}\log K - \log a_{Na^+} \quad (6)$$

For the mafic eclogite, equilibrium between components of omphacitic clinopyroxene, garnet, talc and coesite enables one to write

$$Mg_3Si_4O_{10}(OH)_2 + 2NaAlSi_2O_6 + 2H^+$$
$$= Mg_3Al_2Si_3O_{12} + 5SiO_2 + 2Na^+ + 2H_2O \quad (7)$$

The reaction in equation (7) can be represented by

$$pH = \frac{1}{2}\log K - \log a_{Na^+} \quad (8)$$

Values of $\log K$ in equations (6) and (8) were calculated using standard Gibbs free energies of the aqueous species and those of jadeite, kyanite and coesite[28,30]. These data were used because they explicitly avoid the uncertainties introduced by the lack of an adequate alkali oxide reference basis for the free energies of alkali silicates. Instead, they are based on a combination of experimental data referring to different reaction stoichiometries involving alkali silicates, which enabled a unique set of free energies to be obtained that are in closer agreement with the data of Hemley and colleagues than other thermodynamic treatments. A range of values for the a_{Na^+} from 0.1 to 1.0 was used in equation (3), resulting in the range of estimated pH values. A decrease in the activity of jadeite in equation (4) to 0.5 would produce a decrease in the pH in equation (6) of only 0.15.

The full aqueous speciation and solubility calculations referred to in Figs 3 and 4 were carried out using the computer code EQ3NR adapted for elevated pressures and temperatures with data files generated using the thermodynamic data sources cited above (Supplementary Information).

Received 23 April 2014; accepted 10 October 2014; published online 17 November 2014

References

1. Ague, J. J. & Nicolescu, S. Carbon dioxide released from subduction zones by fluid-mediated reactions. *Nature Geosci.* **7,** 355–360 (2014).
2. Frezzotti, M. L., Selverstone, J., Sharp, Z. D. & Compagnoni, R. Carbonate dissolution during subduction revealed by diamond-bearing rocks from the Alps. *Nature Geosci.* **4,** 703–706 (2011).
3. Manning, C. E. Geochemistry: A piece of the deep carbon puzzle. *Nature Geosci.* **7,** 333–334 (2014).
4. Connolly, J. A. D. Computation of phase equilibria by linear programming: A tool for geodynamic modeling and its application to subduction zone decarbonation. *Earth Planet. Sci. Lett.* **236,** 524–541 (2005).
5. Zhang, C. & Duan, Z. A model for C–O–H fluid in the Earth's mantle. *Geochim. Cosmochim. Acta* **73,** 2089–2102 (2009).
6. Facq, S., Daniel, I. & Sverjensky, D. A. *In situ* Raman study and thermodynamic model of aqueous carbonate speciation in equilibrium with aragonite under subduction zone conditions. *Geochim. Cosmochim. Acta* **132,** 375–390 (2014).
7. Sverjensky, D. A., Harrison, B. & Azzolini, D. Water in the deep Earth: The dielectric constant and the solubilities of quartz and corundum to 60 kb and 1,200 °C. *Geochim. Cosmochim. Acta* **129,** 125–145 (2014).
8. Manning, C. E. Thermodynamic modeling of fluid–rock interaction at mid-crustal to upper-mantle conditions. *Rev. Mineral. Geochem.* **76,** 135–164 (2013).
9. Dasgupta, R. Ingassing, storage, and outgassing of terrestrial carbon through geologic time. *Rev. Mineral. Geochem.* **75,** 183–229 (2013).
10. Evans, K. A. The redox budget of subduction zones. *Earth Sci. Rev.* **113,** 11–32 (2012).
11. Frost, D. J. & McCammon, C. A. The redox state of Earth's mantle. *Annu. Rev. Earth Planet. Sci.* **36,** 389–420 (2008).
12. Pan, D., Spanu, L., Harrison, B., Sverjensky, D. A. & Galli, G. The dielectric constant of water under extreme conditions and transport of carbonates in the deep earth. *Proc. Natl Acad. Sci. USA* **110,** 6646–6650 (2013).
13. Tomlinson, E. L., Jones, A. P. & Harris, J. W. Co-existing fluid and silicate inclusions in mantle diamond. *Earth Planet. Sci. Lett.* **250,** 581–595 (2006).
14. Caciagli, N. & Manning, C. The solubility of calcite in water at 6–16 kbar and 500–800°C. *Contrib. Mineral. Petrol.* **146,** 275–285 (2003).

© 2014 Macmillan Publishers Limited. All rights reserved.

15. Manning, C. E., Shock, E. L. & Sverjensky, D. A. The chemistry of carbon in aqueous fluids at crustal and upper-mantle conditions: Experimental and theoretical constraints. *Rev. Mineral. Geochem.* **75,** 108–148 (2013).
16. Shirey, S. B. *et al.* Diamonds and the geology of mantle carbon. *Rev. Mineral. Geochem.* **75,** 355–421 (2013).
17. Hammouda, T. High-pressure melting of carbonated eclogite and experimental constraints on carbon recycling and storage in the mantle. *Earth Planet. Sci. Lett.* **214,** 357–368 (2003).
18. Hacker, B. R. H_2O subduction beyond arcs. *Geochem. Geophys. Geosys.* **9,** Q03001 (2008).
19. Stagno, V., Ojwang, D. O., McCammon, C. A. & Frost, D. J. The oxidation state of the mantle and the extraction of carbon from Earth's interior. *Nature* **493,** 84–88 (2013).
20. Stagno, V., Frost, D. J. & McCammon, C. A. *AGU Fall Meeting Abstracts* Vol. 1, Abstract no. DI21A-2060 (American Geophysical Union, 2011).
21. Frezzotti, M-L., Huizenga, J-M., Compagnoni, R. & Selverstone, J. Diamond formation by carbon saturation in C–O–H fluids during cold subduction of oceanic lithosphere. *Geochim. Cosmochim. Acta* **143,** 68–86 (2013).
22. Van Keken, P. E., Hacker, B. R., Syracuse, E. M. & Abers, G. A. Subduction factory: 4. Depth-dependent flux of H_2O from subducting slabs worldwide. *J. Geophys. Res.* **116,** B01401 (2011).
23. Stagno, V. & Frost, D. J. Carbon speciation in the asthenosphere: Experimental measurements of the redox conditions at which carbonate-bearing melts coexist with graphite or diamond in peridotite assemblages. *Earth Planet. Sci. Lett.* **300,** 72–84 (2010).
24. Hermann, J., Zheng, Y-F. & Rubatto, D. Deep fluids in subducted continental crust. *Elements* **9,** 281–287 (2013).
25. Ohmoto, H. Systematics of sulfur and carbon isotopes in hydrothermal ore deposits. *Econ. Geol.* **67,** 551–578 (1972).
26. Shock, E. L., Oelkers, E. H., Johnson, J. W., Sverjensky, D. A. & Helgeson, H. C. Calculation of the thermodynamic and transport properties of aqueous species at high pressures and temperatures: Effective electrostatic radii to 1000 °C and 5 kb. *Faraday Soc. Trans.* **88,** 803–826 (1992).
27. Bowers, T. S., Jackson, K. J. & Helgeson, H. C. *Equilibrium Activity Diagrams* (Springer, 1984).
28. Berman, R. G. Internally-consistent thermodynamic data for minerals in the system Na_2O–K_2O–CaO–MgO–FeO–Fe_2O_3–Al_2O_3–SiO_2–TiO_2–H_2O–CO_2. *J. Petrol.* **29,** 445–522 (1988).
29. Holland, T. J. B. & Powell, R. An improved and extended internally consistent thermodynamic dataset for phases of petrological interest, involving a new equation of state for solids. *J. Metamorph. Geol.* **29,** 333–383 (2011).
30. Sverjensky, D. A., Hemley, J. J. & D'Angelo, W. M. Thermodynamic assessment of hydrothermal alkali feldspar–mica–aluminosilicate equilibria. *Geochim. Cosmochim. Acta* **55,** 989–1004 (1991).

Acknowledgements

This research was supported by the WDC Research Fund (V.S.), a Johns Hopkins Graduate Fellowship (F.H.), grants from the Sloan Foundation through the Deep Carbon Observatory (Reservoirs and Fluxes and Extreme Physics and Chemistry programmes to D.A.S.) and grant DOE DE-FG-02-96ER-14616 (D.A.S.). We are also grateful for the help and support of the Johns Hopkins University and the Geophysical Laboratory of the Carnegie Institution of Washington. We wish to acknowledge reviews of the manuscript by R. E. Cohen, R. M. Hazen and C. M. Schiffries, as well as helpful discussions with I. Daniel, Y. Fei, M. S. Ghiorso, R. J. Hemley, S. Lobanov, C. E. Manning, S. Mikhail, B. O. Mysen and E. L. Shock.

Author contributions

All authors contributed to the calculations and the writing of the manuscript. The activity diagrams were calculated by F.H., the aqueous speciation and solubility modelling was carried out by D.A.S. The selection of systems of interest and oxidation states in the mantle were guided and calculated by V.S.

Additional information

Supplementary information is available in the online version of the paper. Reprints and permissions information is available online at www.nature.com/reprints. Correspondence and requests for materials should be addressed to D.A.S.

Competing financial interests

The authors declare no competing financial interests.

© 2014 Macmillan Publishers Limited. All rights reserved.